ICONHIC 2016
1st International Conference on Natural Hazards & Infrastructure
28-30 June, 2016, Chania, Greece

A combined FRP and selective weakening retrofit for realistic pre-1970's RC structures

D. A. Pohoryles[1], T. Rossetto, J. Melo
EPICentre, University College London, U.K.

H. Varum
FEUP, University of Porto, Portugal

ABSTRACT

A large proportion of existing reinforced concrete (RC) buildings is vulnerable to brittle failure mechanisms in earthquakes due to inadequate seismic detailing. Efficient and practical retrofit solutions are required to prevent future losses. To date, most experimental studies in the field of seismic retrofit with fibre-reinforced polymer (FRP) have concentrated on simplified beam-column joint specimens. These often ignore the real practical challenges incurred by the presence of a floor slab and transverse beams in retrofitting deficient specimens. In this study, the results from four cyclic tests on realistic full-scale typical pre-1970's beam-column joints with slabs and transverse beams are presented. Two realistic retrofit schemes using carbon CFRP sheets are proposed. The first scheme aims to improve the ductility of the deficient joint by providing continuity of the column flexural strengthening through the joint. The second scheme includes selective weakening of the slab and aims to relocate the failure mechanism to the beams. The significance of the presence of the slab on the global behaviour of the sub-assembly is confirmed by the experimental findings. The results highlight that the proposed combined retrofit and selective weakening scheme can successfully increase the ductility of the joint by activating deformation in the beams.

Keywords: FRP retrofit, beam-column joint, experimental, existing structures

INTRODUCTION

Past events, such as the 2009 L'Aquila earthquake, have revealed the vulnerability of existing reinforced concrete (RC) structures predating detailed seismic design guidelines (pre-1970's) even to moderate earthquakes (Global Risk Miyamoto 2009). Brittle failures such as weak-column/strong-beam mechanisms, shear failures or column rebar buckling are characteristic inadequacies in the design of these structures (Ricci et al. 2011). A large proportion of the existing building stock is constituted by such vulnerable structures, making rebuilding uneconomical. Repair and retrofit solutions are hence required in order to avoid future failures and reduce significant human and monetary losses.

Next to traditional retrofit methods such as concrete or steel jacketing, repairs and retrofits with fibre reinforced polymers (FRP) are becoming increasingly popular. For example, they have been implemented extensively in the aftermath of the 2009 L'Aquila, Italy, and 2011 Christchurch, NZ, earthquakes. Most FRP retrofit schemes observed in the field address the behaviour of individual members only, but a number of efficient FRP schemes for beam-column joints have been proposed in the literature. The latter typically aim to improve the shear capacity of unreinforced joint panels, improve the bond of beam bars with inadequate anchorage or provide

[1] Corresponding Author: D. A. Pohoryles, *University College London, daniel.pohoryles.10@ucl.ac.uk*

confinement and strengthening to columns to achieve a hierarchy of strengths governed by capacity design principles and hence a more ductile failure mechanism (Bousselham 2010).

A number of FRP retrofit schemes for beam-column joint strengthening have been presented in the literature (e.g.: Akguzel and Pampanin 2012; Antonopoulos and Triantafillou 2003; Del Vecchio et al. 2014). The results from over 30 experimental investigations on the cyclic behaviour of FRP retrofitted non-seismically designed RC joints have been systematically compiled in a database of over 200 specimens (Pohoryles and Rossetto 2014). Review of this database reveals that a majority of experimental specimens tested in the literature have scaled dimensions (61%) and do not contain slabs or transverse beams (88%), despite it being known that both these factors influence the failure mechanism of joints and affect the effectiveness of FRP retrofits (Choudhury et al. 2013; Park and Mosalam 2013). Furthermore, practical challenges to the retrofit solution, such as the location of anchors, wrapping of members and continuity of flexural strengthening are not sufficiently addressed when slabs and transverse beams are ignored. Such specimens hence do not reflect real buildings and real retrofit design situations (ACI 2014).

An initial experimental study on realistic pre-1970's full-scale interior beam-column joints with slab and transverse beams was conducted in order to propose and assess a simple and realistic FRP retrofit solution (Pohoryles et al. 2015b). This initial study demonstrated that an FRP retrofit solution comprised of continuous column strengthening through the slab and confinement of the column plastic hinge zones is effective in preventing brittle single-storey column failures and column rebar buckling. A reversal of the hierarchy of strengths between column and beams was not achieved due to the strong contribution of the slab in negative moment capacity and stiffness impairing the rotation of beams.

In order to improve the local and global behaviour of the retrofitted joints, a combination of a CFRP retrofit with selective weakening (SW) is proposed in this study. SW is a counter-intuitive intervention aiming at achieving the desired global performance by selectively weakening a local member (Ireland et al. 2006). In the proposed combined retrofit and SW scheme, the floor slab contribution is reduced by cutting the slab reinforcement along the plastic hinge zone of the beam. The column is then retrofitted by CFRP confinement wraps and longitudinal sheets to enhance its flexural capacity, while ensuring shear failure and rebar buckling are prevented. The flexural strengthening is applied through the joint by means of vertical FRP strands to connect the bottom and top column and ensure single-storey failure is avoided.

In this paper results from four full-scale cyclic tests on realistic CFRP repaired and retrofitted specimens with and without SW are compared. The effect of the FRP retrofit and SW scheme are assessed in terms of observed failure mechanism and global lateral capacity. The scheme aims at changing the failure mechanism of the joint to a more ductile beam mechanism. The presented experimental results are also used to compare the relative effectiveness of retrofit and repair, as repairing pre-damaged structures is an important aspect. The attainment of the retrofit aims, as well as practical aspects and potential improvements of the retrofit scheme are discussed.

METHODOLOGY

Experimental set-up

Four quasi-static cyclic tests conducted on full-scale RC beam-column joints are presented in this section. These tests are part of a larger, on-going experimental campaign conducted by University College London and the University of Porto in the Laboratory of Aveiro University (Portugal). The loading set-up of the tests is shown in Figure 1. A lateral cyclic displacement protocol (d_c) with three cycles per increment is applied in the superior column at 1.5m from the centre of the joint core. A constant axial load (*N1*) of 425 kN is applied to the top and bottom of the columns. An additional axial load (*N2*) of 25 kN is applied at the bottom to induce reaction forces in the beam supports, simulating moments from gravity loading.

The experiments are monitored using eight strain gauges on the reinforcement (4 on the superior column, one on the inferior column, two on the bottom beam bars and one on the top beam bars), four strain gauges on the vertical FRP, 16 LVDT's, 28 rectilinear displacement transducers, four draw-wire position transducers and four inductive linear position sensors.

Test specimens and materials

The four specimens presented in this study are two control specimens, C1 and C1-sw, and two retrofit specimens, C1-RT-A and C1-RT-A-sw. The specimens labelled 'sw' present selective weakening of the slab. The specimens are designed to represent real-scale interior beam-column joints in a four-storey RC frame structure, as shown in Figure 1. The superior and inferior columns represent a half-storey 1.50m column with a square cross-section of 300 mm by 300 mm. Similarly, each beam represents a 2.00m rectangular half-span beam with a cross-section of 450 mm deep to 300 mm wide. The slab is 1.95 m wide, with a depth of 150 mm.

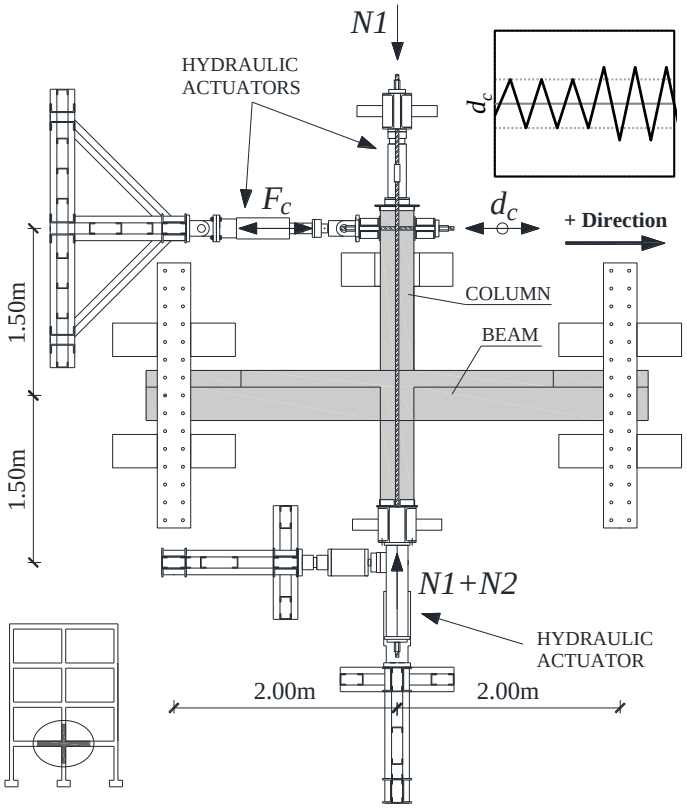

Figure 1. Test-set up, prototype structure and sample of loading protocol.

The reinforcement detailing adopted in all four specimens can be seen in Figure 2. It aims to reflect the common design of a beam-column joint in a pre-1970's reinforced concrete building in the Mediterranean. The limits of the REBA Portuguese code are followed, adopting a seismic coefficient for lateral load of 0.05 of axial load.

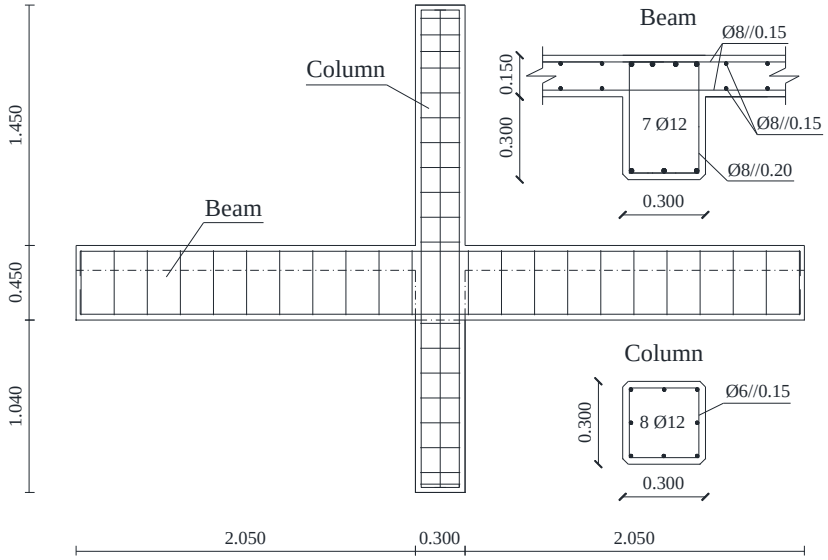

Figure 2. Full-scale beam-column joint specimen reinforcement detailing (in m).

Typical design deficiencies leading to brittle failure mechanisms are related to the specimen's non-compliance with capacity design principles. These include an inappropriate hierarchy of strengths with a lower flexural capacity of the columns than the beams and a low shear capacity of the joint due to the lack of reinforcement in the joint, as well as a lack of confinement in the columns due to inadequate transverse reinforcement spacing.

In order to assess potential failure mechanisms and inform the design of the FRP retrofit schemes, a full non-linear finite element model of the specimens was created (Pohoryles et al. 2015a). Failure in the column in bending with rebar buckling is anticipated. Moreover, due to the contribution of the slab and the asymmetric reinforcement in the beam, less rotation and hence less cracks in the beams are expected.

The mean values of the material properties are summarised in Table 1. Compressive tests of concrete cylinder samples (Ø150 x 300 mm2), as well as tensile strength tests on steel and the CFRP (S&P C-240 sheet) are performed. For the CFRP tensile strength, the testing method in ISO/DIS 10406-2:2013 is adopted. The reported values are f_{cm}, the mean concrete compressive strength of cylinder samples, f_y, the yield strength of reinforcement steel, f_u, the ultimate tensile strength of reinforcement, and $f_{u,FRP}$, $\varepsilon_{u,FRP}$ and t_f, the ultimate strength, strain and thickness of FRP.

Table 1. Material properties for beam-column joint specimens.

Specimen	f_{cm} (MPa)	f_y/f_u - Φ12 (MPa)	f_y/f_u – Φ8 (MPa)	f_y/f_u -Φ6 (MPa)	$f_{u,FRP}$ (MPa)	$\varepsilon_{u,FRP}$ (%)	t_f (mm)
C1	23.4	450/570	540/640	538/645	3300	1.7	0.223
C1-sw	26.0						
C1-RT-A	23.8						
C1-RT-A-sw	22.0						

FRP retrofit schemes

The two retrofit schemes presented in this study are designed to address different targets in terms of cyclic performance. The first scheme (RT-A) aims to improve the strength of the specimen by (i) increasing the moment capacity and ductility of the deficient column and (ii) increasing the global displacement capacity of the specimen by connecting the flexural strengthening of the superior and inferior columns. The second scheme (RT-A-sw) aims to improve the displacement ductility of the specimen by selectively weakening the slab in addition to strengthening the column as in RT-A so as to ensure a ductile beam failure mechanism that follows capacity design principles.

The relative strength of the strengthened members is initially evaluated both by the previously presented FE-modelling and design equations from the CNR-DT/200 (2013), as well as the ACI 440 (2008) guidelines. The main features of the retrofit for both specimens are shown in Figure 3. For C1-RT-A-sw, first, the slab concrete and reinforcement are cut along a length of 600 mm using a circular saw. After surface preparation (roughening) of the concrete and rounding of the edges to a radius of 25 mm, a first layer of 250 mm wide CFRP sheet is then applied, extending 750 mm along the axis of both columns. This aims to increase the flexural capacity of the columns to delay a weak column – strong beam mechanism.

In order to achieve adequate flexural strengthening, it is important to provide continuity in the vertical longitudinal FRP through the joint (ACI 2014). By means of continuous strengthening, the FRP on the columns above and below the joint are activated, which results in more symmetric behaviour of the two columns. This in turn enables higher levels of drift to be achieved by the structure as single-storey failure mechanisms are avoided. This is, however, a difficult task for realistic interior joints with slab and has only been addressed by very few experimental campaigns (e.g.: Shiohara et al. 2009). In both schemes CFRP sheets are rolled into strands and glued together using epoxy. These 'strands' are then passed through plastic tubes placed in holes through the slab at the corners of the columns. The ends of the strands are played out and glued onto the columns to serve as fan-type anchors, with additional anchorage provided by steel plates. A total of 6 equivalent layers of flexural strengthening are applied through the strands in RT-A (two 750mm wide sheets used as strands), while only 4 layers are used in RT-A-sw (two 500 mm wide sheets) due to the weakening of the slab.

Finally, horizontal FRP wraps are applied to anchor the splayed-out strands, as well as to provide confinement and shear strengthening of the columns. Close to the joint, three layers of 250 mm wide confinement CFRP are applied, above, two layers of 500 mm wide CFRP are required.

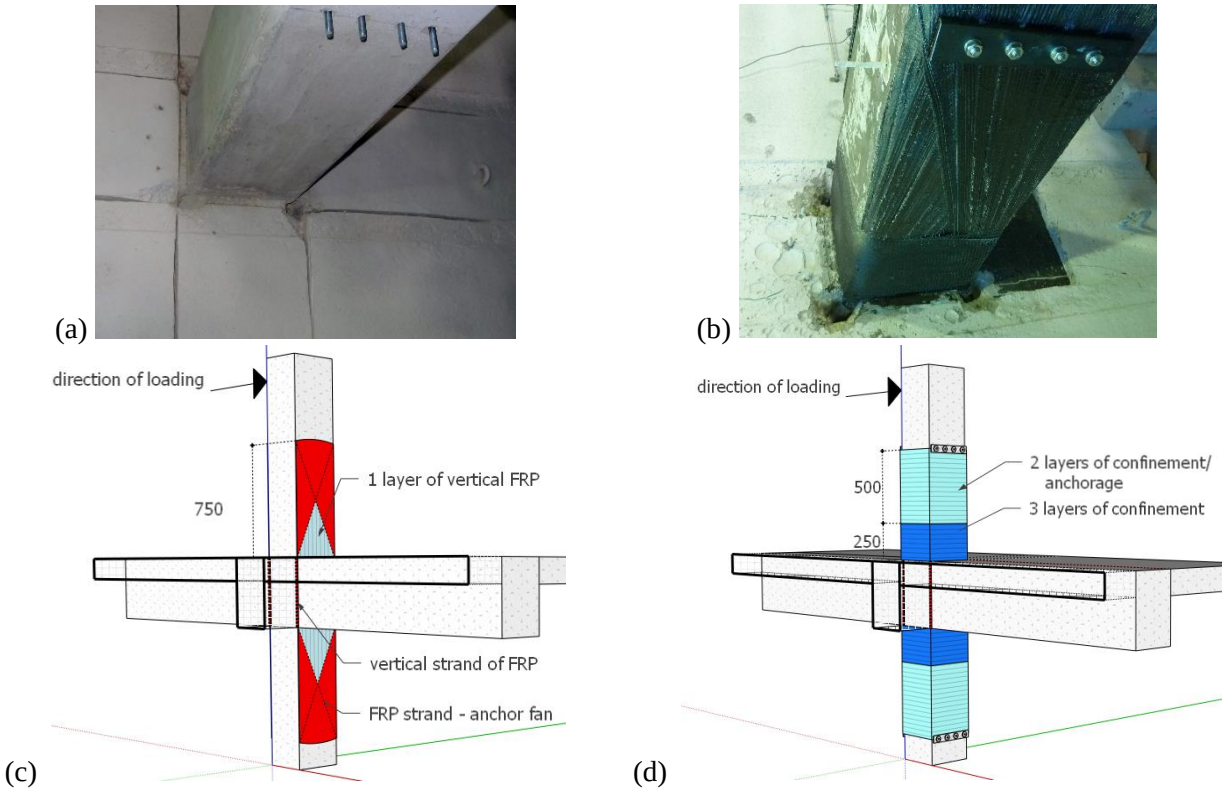

Figure 3. (a) Selective weakening cuts; (b) Applied retrofit FRP strands, anchors and first layer of confinement. (c) First steps of retrofit; (d) final stage of retrofit.

RESULTS

The results from the four full-scale tests are presented here. The global behaviour in terms of lateral force–displacement relationships, as well as the local behaviour in terms of moment-curvature plots for individual members is analysed. A summary of the results is presented in Table 2.

Table 2. Summary of main experimental results (difference to C1 in brackets).

Specimen	**F_{max}** (kN)	**Failure location**	Δ_y (%)	$\mu_{\Delta u}$	**Dissipated Energy** (kN.m)	**PPS** (kN/mm)	**ICSD max.** (%)	$\varepsilon_{FRP,max}$ **strand** (%)
C1	63.1	Superior Column	0.65	3.6	32.1	-0.49	-23.22	
C1-sw	67.5 (+7.0%)	Superior Column	0.48	3.9 (+7.5%)	22.7 (-29.4%)	-0.4 (-18%)	-27.9 (+20%)	
C1-RT-A	87.7 (+39.1%)	Both Columns	0.83	6.3 (+74.6%)	93.8 (+192.5%)	-0.33 (-34%)	-10.9 (-53%)	0.14
C1-RT-A-sw	71.6 (+13.5%)	Beams, Joint	0.78	6.7 (+84.9%)	94.5 (+194.7%)	-0.17 (-66%)	-13.9 (-40%)	0.26

Yield drift, Δ_y, is defined as the drift at which the first strain gauge reading exceeds the steel yield strain (0.2%) and the ultimate drift, Δ_u, is determined when a strength reduction of 20% (F_u) from the maximum force (F_{max}) is achieved (Park et al. 1987). The ultimate displacement ductility, $\mu_{\Delta u}$, is defined as the ratio between Δ_u and Δ_y. The post-peak softening slope (PPS) is defined as the slope between F_{max} and F_u, and provides an indication of the residual strength of the structure. The global energy dissipation is defined as the integral of the force-displacement curve and the energy dissipated by individual members (columns and beams), is calculated from the moment-rotation curves along the length of the members. Finally, the inter-cycle strength degradation

(ICSD) is looked at as a measure of a structure's behaviour upon repeated cyclic loading and is defined here as the reduction in strength at the end of the 1st and 2nd cycles at each drift level.

Control specimens

The global behaviour of both control specimens with pre-1970's reinforcement detailing is, as expected, characterized by a single-storey failure, dominated by a large deformation of the superior columns, with very limited rotation of the joint, inferior column and beams. A relatively low peak lateral force of 63.1 kN and 67.5 kN are achieved, respectively.

The final damage state of C1 and C1-sw are shown in Figure 4, highlighting that damage and cracking are confined to the plastic hinge zone of the superior column. Yielding of rebars is only observed in the longitudinal reinforcement above the joint at a yield drift of 0.65%. Due to the low rotation of beams, no yield of beam bars is observed. After plastic hinge formation, the ultimate state is reached by concrete crushing and buckling of the column bars just above the column-joint interface. The ultimate displacement ductility is 3.6 for C1 and 3.9 for C1-sw.

(a) (b)

Figure 4. Final damage state in (a) C1 and (b) C1-sw.

Overall, selective weakening of the slab alone does not significantly alter the specimen's behaviour, as the same failure mechanism is observed in both control specimens. The weak-column strong-beam strength hierarchy is unaffected by the cuts in the slab, as the columns remain the weakest member. The slight increase in strength (6.96 %) and ductility (7.47%) can be attributed to the higher concrete strength in C1-sw. A similar post-peak softening behaviour and strength degradation between cycles is also recorded. However, a reduction in the total cumulative dissipated energy is observed, possibly due to removal of slab contribution.

Retrofit specimens

The final damage states for both retrofitted specimens are shown in Figures 5 and 6. For both specimens an improved seismic behaviour compared to C1 and C1-sw is observed, with more damage in the beams and no debonding or rupture of the CFRP. For C1-RT-A-sw, as expected, an increased strain in the FRP strands (0.26%) compared to C1-RT-A (0.14%) is recorded due to the smaller amount of FRP in the strands.

For specimen C1-RT-A, large cracks at the slab-column and beam- inferior column interfaces are noticed. The failure mechanism ultimately involves both columns, eliminating the single-storey mechanism of C1, as shown conceptually in Figure 5 (c). As a consequence, compared to the control specimens, yield is delayed significantly, as a higher value of drift is necessary to achieve the same curvature in the column. Buckling of the column bars is also successfully prevented. As can be seen from the envelope curves in Figure 7, specimen C1-RT-A presents a much larger failure load (+39.1%) and ultimate drift than C1, leading to a ductility of 6.3 (+74.6%). The larger lateral load can be ascribed to the increase in moment capacity of the column from 90 kNm in C1 to 115 kNm in C1-RT-A due to the FRP strands. The larger ductility is attributable to a combination of increased confinement through the FRP wraps and the aforementioned failure mechanism involving both columns rather than a single column, with quasi-symmetric rotation of the superior and inferior columns throughout the test.

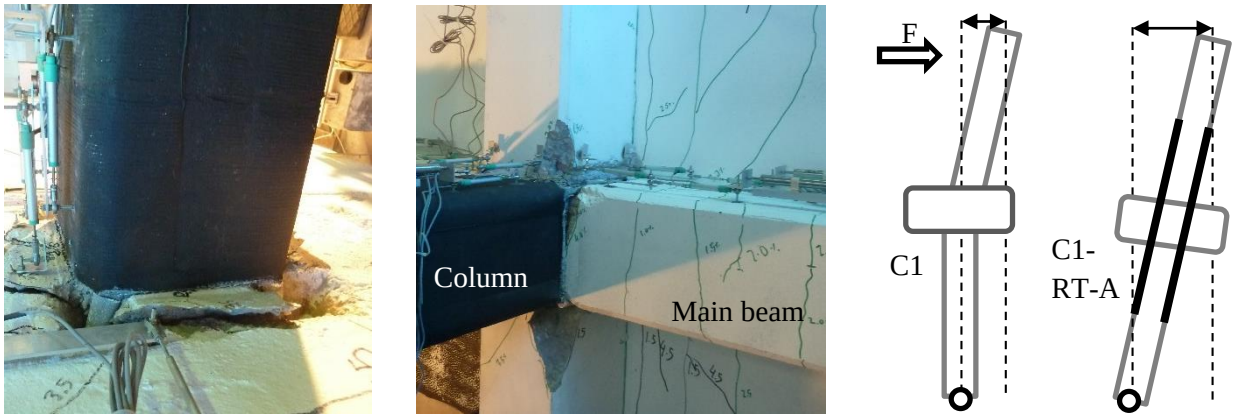

(a) (b) (c)

Figure 5. Final damage in C1-RT-A (a) superior and (b) inferior storey; (c) schematic failure mechanism

Due to the higher capacity of the retrofitted columns, the rotation in the beam is also observed to increase, leading to larger curvatures and damage in the bottom face of the beams, which are not observed in C1 and C1-sw. Failure is however not governed by the beams, and this can be explained by the slab providing a high stiffness and added capacity to the top of the beam, limiting its rotation, as shown in Figure 8 (b).

For C1-RT-A-sw, a change in hierarchy of strengths is anticipated, resulting in a failure mechanism governed by the beams and joint. Cracks in the bottom and top face of the beams, shown in Figure 6 (b), are observed at lower drift levels (0.5%) compared to C1-RT-A (1%). In the columns, no cracks are detected after removal of the FRP, however, some cracks in the joint are noticeable after removal of the transverse beams (Figure 6 (c)).

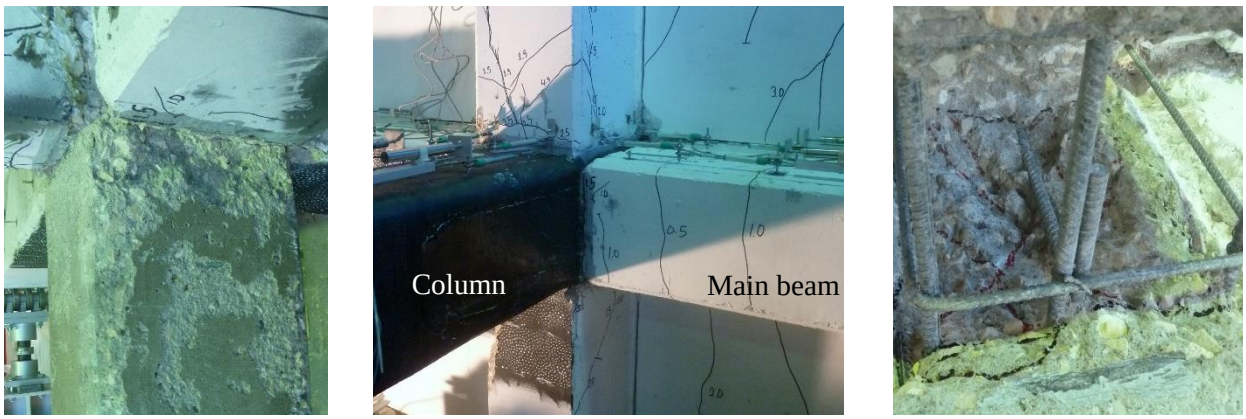

(a) (b) (c)

Figure 6. Final damage state in C1-RT-A-sw: (a) No cracks in column after removal of FRP; (b) early cracks in main beam; (c) damage in joint visible after removal of transverse beam

As shown in Figure 7, the increase in lateral load is less significant (+13.52 %) then for C1-RT-A (+39.05%). A slightly higher displacement ductility is however observed for C1-RT-A-sw (6.69) compared to C1-RT-A (6.32), which is significantly larger compared to C1 in both cases (84.8% and 74.6% increase, respectively). Similarly, the dissipated energy for both retrofits reaches nearly three times the energy dissipated in C1.

The improved failure mechanism in C1-RT-A-sw is also noticeable in the significantly improved post-peak softening behaviour. The softening slope is reduced by 66% for C1-RT-A-sw, compared to 34% in C1-RT-A and 18% in C1-sw. Similarly, the strength degradation between cycles is improved by over 40% in both retrofit specimens.

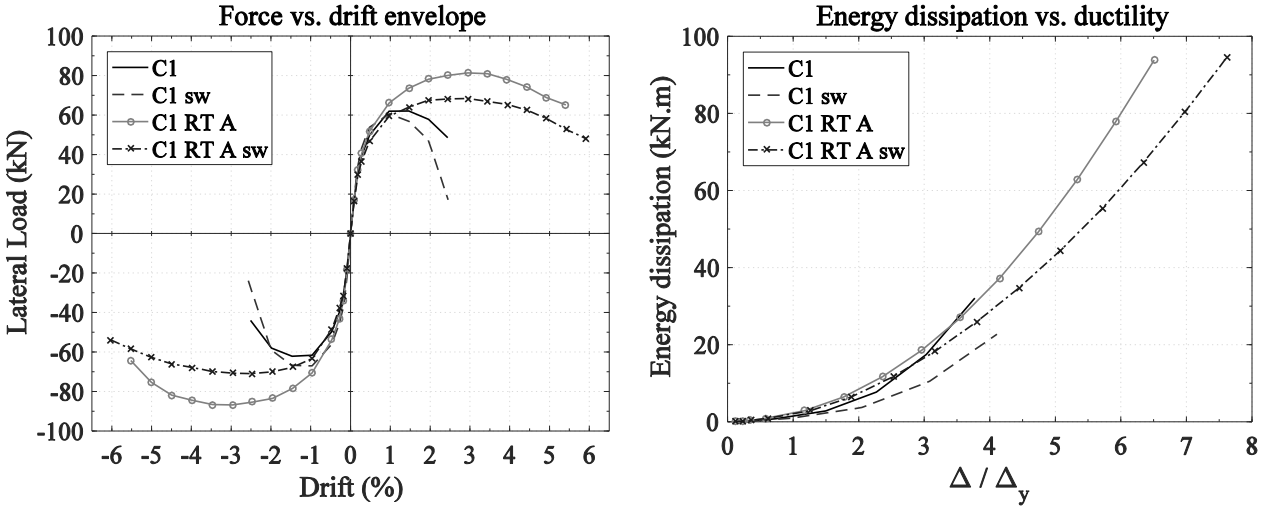

Figure 7. Force-drift envelope and energy dissipation against ductility for all specimens (Δ_y, yield drift)

The change in failure mechanism for specimen C1-RT-A-sw is further demonstrated by a much higher beam and joint participation to the total energy dissipation. As shown in Figure 8 (a), for the control specimens over 80% and for C1-RT-A over 70% of the total energy dissipation is dissipated by the column. This is reduced to 49 % in C1-RT-A-sw, with 27% of due to the beams. Moreover, for C1-RT-A-sw, a much larger curvature in the top face of the beam is observed in Figure 8 (b) due to the selective weakening of the slab. A more symmetric rotation of the beam in positive and negative drift directions and hence a larger beam participation to the global behaviour are observed. This is paired with lower column curvatures recorded at each drift level for C1-RT-A-sw, with cracks at the column-slab interface occurring at lower drift levels for C1-RT-A.

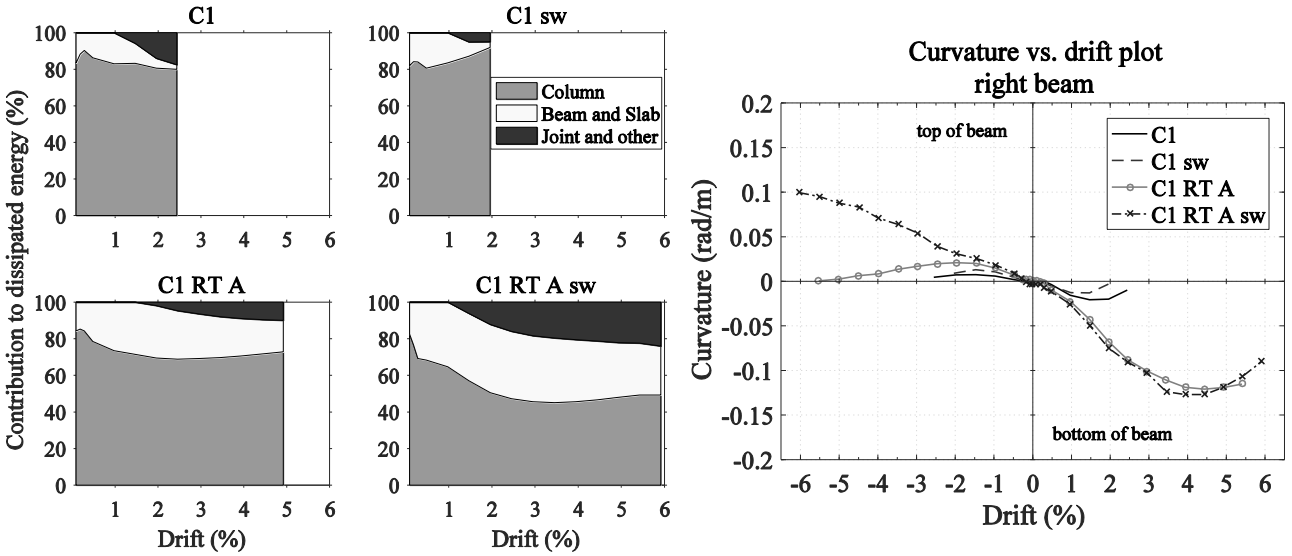

Figure 8. (left) Contribution to energy dissipation by members for all specimens
(right) Beam curvature-drift envelope

CONCLUSIONS

The results from four interior full-scale beam-column joint tests with slab and transverse beams are presented in this paper. Two realistic FRP retrofit strategies for specimens with typical pre-1970's deficiencies are proposed and tested. The non-seismically designed control specimens exhibit non-ductile single storey failure that is prevented in both proposed retrofit strategies, which proved an enhanced flexural capacity of the columns and prevent buckling of the column bars. Full continuity of the flexural strengthening is achieved using the proposed FRP strands. The combination of fan-shaped splaying of the strands, mechanical anchorage with steel plates and FRP anchorage with horizontal wraps proves successful in avoiding significant debonding.

The test outcomes highlight the importance of considering the slab when assessing the behaviour of retrofitted beam-column joints. The experimental results confirm previous observations on the significance of slabs (Park and Mosalam 2013). Retrofit RT-A achieves a failure mechanism with significant strength enhancement and energy dissipation. RT-A however does not result in a desirable failure mechanism as the columns still dominate the behaviour. RT-A-sw is instead successful in reversing the failure to be concentrated in the beams. Increased beam rotation, in particular in the top side, and an increased contribution to the energy dissipation by the beams are observed and demonstrate that selective weakening is successful in ensuring a failure mechanism governed by the beams. The low increase in strength in C1-RT-A-sw and slight damage in the joint, however leave room for improvement in future retrofit designs. As the failure is governed by the strength of the beams and joint, future FRP retrofits need to apply FRP strengthening of the joint and the beams in order to achieve a ductile failure in the beams with increased lateral load capacity.

Overall, the practical FRP retrofit schemes presented in this study successfully take into account the realistic geometric challenges of a structure and are hence applicable to real buildings. The proposed and implemented retrofit solutions provide very satisfactory improvements of the behaviour of the as-built specimens. An improved ductile and dissipative behaviour is achieved globally, with significant improvements in local rotations of members for both retrofits.

ACKNOWLEDGMENTS

This research is funded as part of the Challenging RISK project funded by EPSRC (EP/K022377/1). The authors acknowledge the staff of the Civil Laboratory at the University of Aveiro for the support during the experimental campaign. The CFRP used in the experiments is kindly provided by S&P reinforcement.

REFERENCES

ACI. 440.2R-08 - Guide for the design and construction of externally bonded FRP systems for strengthening concrete structures. American Concrete Institute, Farmington Hills, Mich, 2008.

ACI. 440-F - Seismic Strengthening of Concrete Buildings Using FRP (draft). American Concrete Institute, 2014.

Akguzel U, Pampanin S. Assessment and Design Procedure for the Seismic Retrofit of Reinforced Concrete Beam-Column Joints using FRP Composite Materials. *Journal of Composites for Construction*, 2012, 16(1): 21–34.

Antonopoulos C, Triantafillou T. Experimental Investigation of FRP-Strengthened RC Beam-Column Joints. *Journal of Composites for Construction*, 2003, 7(1): 39–49.

Bousselham A. State of Research on Seismic Retrofit of RC Beam-Column Joints with Externally Bonded FRP. *Journal of Composites for Construction*, 2010, 14(1): 49–61.

Choudhury AM, Deb SK, Dutta A. Study on size effect of fibre reinforced polymer retrofitted reinforced concrete beam–column connections under cyclic loading. *Canadian Journal of Civil Engineering*, 2013, 40(4): 353–360.

CNR. DT 200.R1/2013 - Guide for the Design and Construction of Externally Bonded FRP Systems for Strengthening Existing Structures - Materials, RC and PC structures, masonry structures. CNR, 2013.

Del Vecchio C, Di Ludovico M, Balsamo A, Prota A, Manfredi G, Dolce M. Experimental Investigation of Exterior RC Beam-Column Joints Retrofitted with FRP Systems. *Journal of Composites for Construction*, 2014, 18(4).

Global Risk Miyamoto. M6.3 L'Aquila, Italy, Earthquake Field Investigation Report, 2009.

Ireland MG, Pampanin S, Bull DK. Concept and Implementation of a selective Weakening Approach for the Seismic Retrofit of RC buildings. *NZSEE Conference*, New Zealand, 2006.

Park S, Mosalam KM. Experimental Investigation of Nonductile RC Corner Beam-Column Joints with Floor Slabs. *Journal of Structural Engineering*, 2013, 139(1): 1–14.

Park YJ, Ang AH, Wen YK. Damage-limiting aseismic design of buildings. *Earthquake spectra*, 1987, 3(1): 1–26.

Pohoryles DA, Melo J, Rossetto T. Numerical modelling of FRP-strengthened RC beam-column joints. *SECED Conference*, Cambridge, UK, 2015a.

Pohoryles DA, Melo J, Rossetto T, Varum H. Experimental investigation on the seismic FRP retrofit of full-scale RC joints. *Improving the Seismic Performance of Existing Buildings and Other Structures*, California, 2015b, 619–631.

Pohoryles DA, Rossetto T. A critical evaluation of current design guidelines for the seismic retrofit of beam-column joints with FRP. *2nd European Conference on Earthquake Engineering and Seismology*, Istanbul, Turkey, 2014.

Ricci P, De Luca F, Verderame GM. 6th April 2009 L'Aquila earthquake, Italy: reinforced concrete building performance. *Bulletin of Earthquake Engineering*, 2011, 9(1): 285–305.

Shiohara H, Kusuhara F, Tajiri S, Fukuyama H. Seismic Retrofit of RC Beam-Column Joints with CFRP Composites. *Improving the Seismic Performance of Existing Buildings and Other Structures*, California, 2009, 1449–1459.